INVITED PRESENTATION

Extreme midinfrared nonlinear optics in semiconductors

J. Kono[1] ***and A.H. Chin***[2*]

[1] *Department of Electrical and Computer Engineering, Rice University, Houston, Texas U.S.A.*
[2] *Lawrence Livermore National Laboratory, Livermore, California U.S.A.*

Abstract. We have observed extreme nonlinear optical phenomena produced by intense midinfrared (MIR) pulses in semiconductors. These phenomena include coherent bandgap distortion (induced sub-bandgap absorption that extends $\sim$ 1 eV below the bandgap), multiple off-resonance optical sidebands (up to $\pm$ 3 MIR photons interacting with a NIR photon), multiple MIR harmonics (up to the seventh harmonic), and significant broadening and modification of MIR harmonic spectra. These observations were made possible by the use of small energy photons, which help minimize interband absorption and sample damage while employing the low dispersion existing at longer wavelengths and maximizing the ponderomotive potential

Introduction

Matter in the presence of an AC electric field of sufficient field strength exhibits phenomena that cannot be understood by treating the field as a small perturbation, i.e., non-perturbative phenomena. The advent of ultrafast sources for intense midinfrared (MIR) or far-infrared (FIR) radiation has opened up the possibility of exploring new regimes of nonlinear optics in semiconductors. The small photon energies help minimize interband absorption and sample damage, while the low dispersion existing at longer wavelengths allows phase-matching over longer distances. Also, for a given laser intensity, the ponderomotive potential of the driven electron increases quadratically with decreasing photon energy [see Eq. (1) below]. Thus, strong-field physics in solids are more suitably studied using MIR or FIR rather than optical or near-infrared (NIR) wavelengths.

This paper describes our recent observations of extreme nonlinear optical behavior in semiconductors in the presence of intense MIR laser pulses from an optical parametric amplifier [1-3]. The phenomena described include: 1) MIR-laser-induced coherent bandgap distortion, i.e., induced absorption that extends $\sim$ 1 eV below the band edge, 2) high-order multiple photon processes, i.e., sideband and harmonic generation, and 3) harmonic-continuum generation as a combined result of self-phase modulation and cross-phase modulation.

Experimental Methods

The source of intense pulses used for these extreme MIR nonlinear optics studies is an optical

*Present address: UltraPhotonics, Fremont, California 94538, U.S.A.

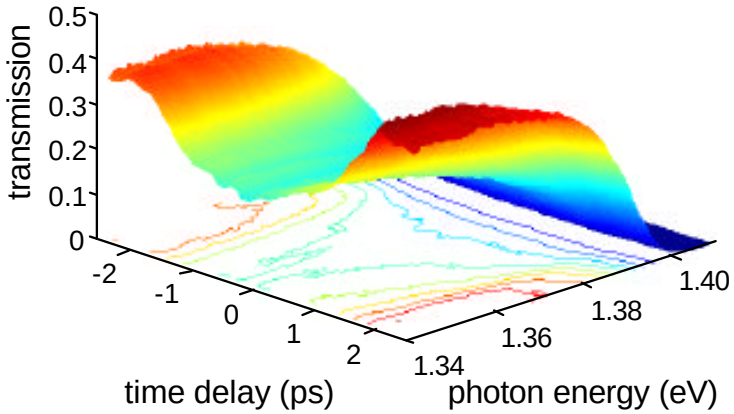

Figure 1. Transmission of a NIR broadband probe pulse through GaAs as a function of time delay between the arrival of the intense 3.5 μm MIR driving pulse and the NIR probe pulse

parametric amplifier (OPA) pumped by a Ti:Sapphire based regenerative amplifier. The system produced pulses at a 1 kHz repetition rate with either $\sim$ 1 ps or $\sim$ 200 fs pulse duration, and (with difference-frequency mixing of the signal and idler) wavelengths from 3 μm to 10 μm. For these studies, we used pulses at wavelengths of 3.5 μm or 6.2 μm (where atmospheric absorption is negligible).

To study laser-induced coherent bandgap distortion, we measured the transmission near the band edge of semiconductors using broadband light as a probe. The broadband light was produced by continuum generation in a sapphire plate, using the residual pump pulse after the OPA. The probe was temporally overlapped with the MIR pump. The probe and pump were focused onto the sample using an off-axis paraboloid. After passing through the sample, the spectrum of the probe was dispersed using a monochromator and detected using a Si CCD camera. Spectra were obtained with the pump at various time delays with respect to the probe, and were subsequently normalized to the probe spectrum without the sample to obtain the absolute transmission (accurate to $\pm$ 5%).

We studied two types of high-order multi-photon processes: sideband and harmonic generation. In sideband generation we measure the NIR spectrum after nonlinear wave mixing of intense NIR and MIR pulses in a semiconductor. Temporal overlap was achieved by varying the optical path of the MIR beam with respect to the NIR beam. In harmonic generation we measured the spectrum of intense MIR pulses after transmission through a semiconductor.

Experimental Results and Discussion

Coherent Bandgap Distortion. Shown in Fig. 1 is transmission data taken using a 3.5 μm MIR driving field with $\sim$ 1 ps pulse duration and $\sim 2\times10^{10}$ W/cm^2 peak incident intensity. Under these conditions, we observed a dramatic *decrease* in transmission that extends past 0.2 eV below the band edge (E_{gap} = 1.4 eV) of the GaAs sample. The energy range over which the change occurs is larger than any observed electro-absorption using strong static fields or energy shift due to intense laser pulses via the AC Stark effect [4]. This induced absorption occurs only during the presence of the intense MIR pulse, clearly demonstrating that no MIR excitation of carriers across the band gap and/or lattice-heating effects are involved.

Shown in Fig. 2(a) is the wavelength dependence of the effect in GaAs, comparing the 3.5 μm case and the 6.2 μm case with $\sim 3\times10^{9}$ W/cm^2 peak incident intensity. Here, we observe

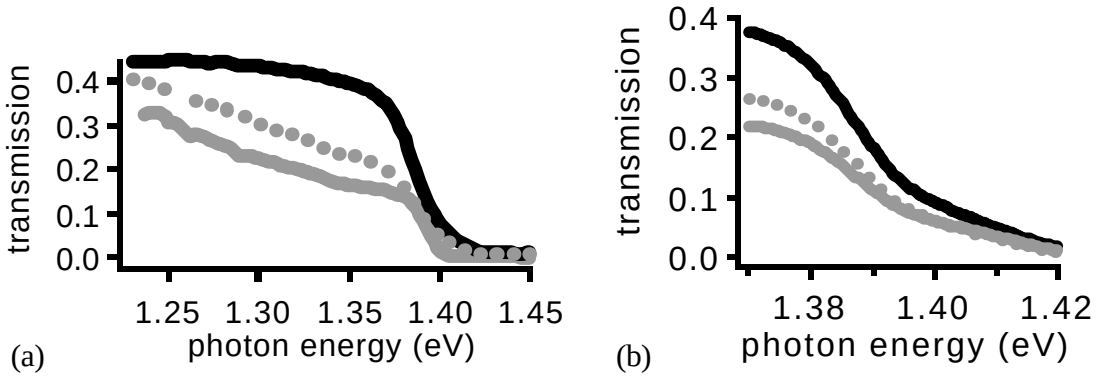

Figure 2. (a) Wavelength dependence of electro-absorption in GaAs: 3.5 μm MIR driving pulse (gray), 6.2 μm MIR driving pulse (gray dashed), and no driving pulse (black). (b) Intensity dependence: I_0 (gray), $I_0/2$ (gray dashed), and with no driving pulse (black)

an effect in the 6.2 μm case that is comparable to the 3.5 μm case, but the cutoff occurs closer to the band edge, due to the smaller MIR photon energy. Shown in Fig. 2(b) is the intensity dependence of the effect using 3.5 μm MIR driving pulses, which is consistent with an absorption coefficient that is linearly dependent on the driving field intensity. Finally, the effect is not specific to GaAs, as we also observed induced absorption in ZnSe (E_g = 2.7 eV) and ZnTe (E_g = 2.3 eV). The induced absorption in ZnSe with and without the presence of a 3.5 μm MIR field is shown in Fig. 3. Our measurements clearly demonstrate not only the magnitude of the effect, but also the extent ($\sim$ 1 eV below the band edge) of the induced absorption, which far exceeds any previously observed induced absorption in semiconductors.

A measure of the field strength required to observe non-perturbative phenomena is the ponderomotive potential (also known as the wiggle or quiver energy), i.e., the time-averaged kinetic energy of an electron in an AC electric field. For a driving AC electric field with vector potential $\vec{A} = \vec{A}_0 e^{i\omega t}$, the ponderomotive potential is given by

$$U_p = \frac{e^2 A_0^2}{4mc^2} = \left(\frac{2\pi e^2}{mc}\right)\left(\frac{I}{\omega^2}\right), \tag{4.1}$$

where *I* is the intensity of the electric field at frequency ω, and *m* is the mass of the electron. Existing models predict a laser-induced absorption with an absorption coefficient that is linear with the ponderomotive potential (or the driving field intensity) and with an extent that is on the order of the ponderomotive potential (or photon energy, since $U_p \sim \hbar\omega$ in our experiments) below the band edge [5]. Both of these predictions are consistent with our data.

Multiple-Photon Phenomena. Typical sideband generation data is shown in Fig. 4. Here, the 800 nm (1.55 eV) NIR probe pulse spectrum is significantly modified in the presence of intense MIR fields to possess multiple sidebands that are spaced by the MIR photon energy. The data in Fig. 4 was obtained in ZnSe using $\sim$ 1 ps pulses of either 3.5 μm wavelength (0.35 eV) with peak intensity of $\sim 2\times10^{10}$ W/cm^2 or 6.2 μm wavelength (0.22 eV) with peak intensity of $\sim 3\times10^{9}$ W/cm^2. We observed sum-frequency and difference-frequency mixing ($\pm$ 1 MIR photon sidebands) as well as higher-order wave mixing, with up to $\pm$ 3 MIR photon sidebands (with

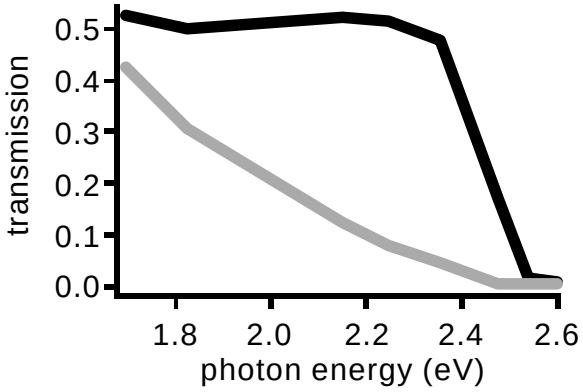

Figure 3. Transmission below the band edge of ZnSe with (gray) and without (black) an intense 3.5 μm MIR driving field

6.2 μm MIR pulses) observed in the spectral range of the detectors used. Previous studies of sideband generation in semiconductors relied on *resonant* enhancement of the nonlinear optical susceptibility [6]. Here, we observed multiple *non-resonant* sidebands in semiconductors. The $\pm$ 1 ($\pm$ 2) MIR photon sidebands are linearly (quadratically) dependent on the MIR intensity up to the maximum MIR intensity used in these experiments.

Figure 5 shows the sideband spectra as a function of time delay in ZnSe for the $\pm$ 1 MIR sidebands. The sideband spectra change in both intensity and peak location as the NIR pulse interacts with different temporal sections of the MIR pulse.

Figure 6(a) shows the multiple harmonics observed in ZnS. While third and higher harmonics have been observed from solid surfaces [7], and MIR harmonics have been observed in gases [8] and liquids [9], we observed multiple (up to fifth) MIR harmonics in *bulk* semiconductors. With higher MIR intensity using shorter ($\sim$ 200 fs) pulses, we also observed an interesting broadening. An extreme case is shown in Fig. 6(b), where multiple (up to seventh) MIR harmonics are seen to exhibit both spectral broadening and overlap between the harmonics to form what we refer to as a harmonic-continuum.

Several factors contribute to the generation of the observed extreme nonlinear optical phe-

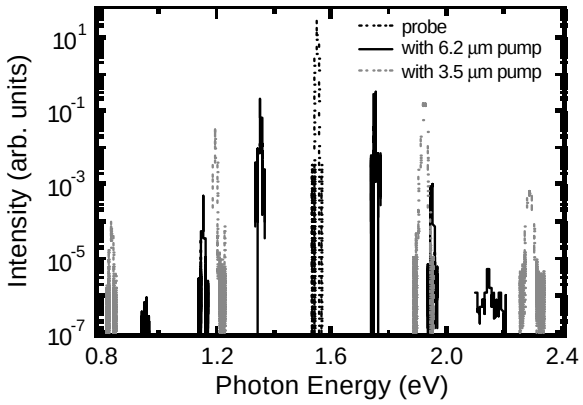

Figure 4. Optical sidebands in polycrystalline ZnSe generated when a MIR pump pulse and a 800 nm (1.55 eV) probe pulse (dashed line) are overlapped

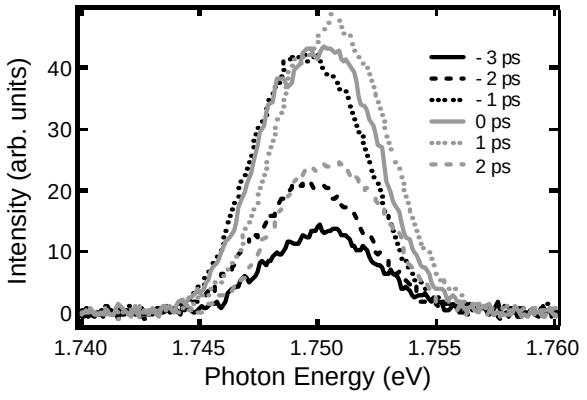

Figure 5. -1 sideband spectra in polycrystalline ZnSe for different time delays between 6.2 μm (0.22 eV) MIR pulses at $\sim 3\times10^9$ W/cm^2 and 800 nm (1.55 eV) NIR pulses

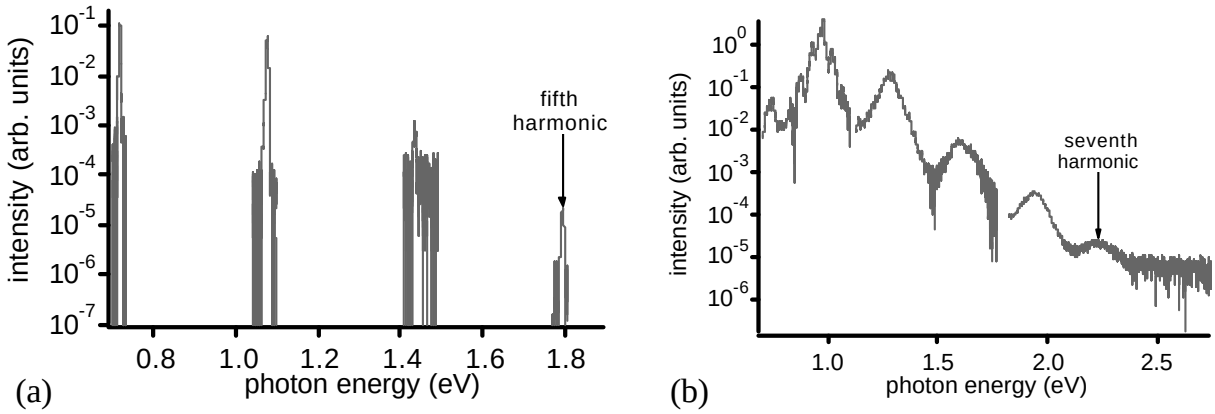

Figure 6. (a) MIR harmonics in ZnS using 3.5 μm (0.35 eV), $\sim$ 1 ps, $\sim 2\times10^{10}$ W/cm^2 MIR pulses. (b) MIR harmonics in ZnSe using $\sim$ 3.9 μm (0.32 eV), $\sim$ 200 fs, $\sim 10^{11}$ W/cm^2 MIR pulses

nomena by minimizing phase mismatch between the beams. Two such factors are the low dispersion that exists at wavelengths in between phonon absorption and interband absorption and the long wavelengths used. Low dispersion allows a longer interaction length for sideband/harmonic generation. Longer wavelengths intrinsically yield longer interaction lengths due to the slower phase variation. Consequently, the generation of sidebands/harmonics is more efficient at longer wavelengths. In spite of these factors, the estimated interaction lengths ($\sim$ 10 μm) are still much shorter than the sample thicknesses used here ($\sim$ 1 mm). Thus, without any spectral modifications, significant phase mismatch exists in the samples.

One factor that can alleviate the remaining phase mismatch is the influence of self-phase modulation (SPM) of the fundamental on sideband/harmonic generation, which is known as cross-phase modulation (XPM) [10]. SPM generates additional bandwidth in the fundamental, which alleviates any strong thickness dependence of phase matching through XPM by providing a distribution of wavevectors that contributes to each sideband/harmonic wavelength. This consequence of XPM, in combination with the low dispersion and long wavelength light used, allows multiple sideband/harmonic generation to be more easily observable using MIR rather than visible fundamental frequencies. To verify this, we performed numerical calculations [3]. We obtained good agreement between the calculations and the data.

Summary

We have observed extreme nonlinear optical phenomena in semiconductors using intense MIR radiation from an optical parametric amplifier. These phenomena include: 1) MIR-laser-induced ultrafast sub-bandgap absorption that extends $\sim$ 1 eV below the band edge, 2) high-order multiple photon processes, i.e., sideband and harmonic generation, involving up to seven photons, and 3) significant spectral broadening and modulation of sidebands and harmonics as a combined result of self-phase modulation and cross-phase modulation. The extreme example of 3) is the appearance of a super-continuum whose spectral width was $\sim$ 2.5 eV. These studies represent the first observations of non-resonant nonlinear optical phenomena in solids in the non-perturbative regime.

Acknowledgments

We gratefully acknowledge support from NSF DMR-0049024, ONR N00014-94-1-1024, the Japan Science and Technology Corporation PRESTO Program, and the NEDO International Joint Research Grant Program. We thank J. M. Bakker, Dr. T. Kimura, A. P. Mitchell, and J. Guo for their assistance with the experiments, Dr. O. G. Calderon for performing simulation calculations, and Prof. H. A. Schwettman and Prof. T. I. Smith for their support.

References

[1] A. H. Chin, J. M. Bakker, and J. Kono, Phys. Rev. Lett. **85**, 3293 (2000)

[2] A. H. Chin, O. G. Calderon, and J. Kono, Phys. Rev. Lett. **86**, 3292 (2001)

[3] O. G. Calderon, A. H. Chin, and J. Kono, Phys. Rev. A **63**, 053807 (2001)

[4] A. Mysyrowicz *et al.*, Phys. Rev. Lett. **56**, 2748 (1986)

[5] Y. Yacoby, Phys. Rev. **169**, 610 (1968); L. C. M. Miranda, Solid State Commun. **45**, 783 (1983); Yu. I. Balkarei and E. M. Epshtein, Sov. Phys. Solid State **15**, 641 (1973); O. A. C. Nunes, J. Appl. Phys. **58**, 2102 (1985); K. Johnsen and A.-P. Jauho, Phys. Rev. B **57**, 8860 (1998)

[6] J. Kono *et al*., Phys. Rev. Lett. **79**, 1758 (1997); C. Phillips *et al*., Appl. Phys. Lett. **75**, 2728 (1999)

[7] Y.-S. Lee, M. H. Anderson, and M. C. Downer, Opt. Lett. **22**, 973 (1997); T. Tsang, Phys. Rev. A **54**, 5454 (1996)

[8] B. Sheehy *et al*., Phys. Rev. Lett. **83**, 5270 (1999)

[9] R. Z*ü*rl and H. Graener, Appl. Phys. B **66**, 213 (1998)

[10] A. M. Zheltikov, N. I. Koroteev, and A. N. Naumov, JETP **88**, 857 (1999); P. P. Ho *et al*., Appl. Phys. Lett. **54**, 111 (1989); H. J. Bakker *et al*., Phys. Rev. A **42**, 4085 (1990)